International Journal of Biological Macromolecules 107 (2018) 949–956

Contents lists available at ScienceDirect

International Journal of Biological Macromolecules

journal homepage: www.elsevier.com/locate/ijbiomac

A combined experimental and molecular simulation study of factors influencing interaction of quinoa proteins–carrageenan

Natalia Montellano Duran[a], Darío Spelzini[a,b], Natael Wayllace[a], Valeria Boeris[a,b], Fernando L. Barroso da Silva[c,d,e,*]

[a] Universidad Nacional de Rosario-CONICET, Facultad de Ciencias Bioquímicas y Farmacéuticas, Área Fisicoquímica, Argentina
[b] Universidad Católica Argentina, Facultad Católica de Química e Ingeniería del Rosario, Argentina
[c] University of São Paulo, School of Pharmaceutical Sciences at Ribeirão Preto, Department of Physics and Chemistry, Brazil
[d] UCD School of Physics, UCD Institute for Discovery and CECAM-IRL, Ireland
[e] Department of Chemical and Biomolecular Engineering, NCSU, USA

ARTICLE INFO

Article history:
Received 2 June 2017
Received in revised form 29 August 2017
Accepted 18 September 2017
Available online 21 September 2017

Keywords:
Quinoa proteins
Carrageenan
Complex formation

ABSTRACT

The interaction between quinoa proteins isolate (QP isolate) and the negatively charged polysaccharide ι-Carragennan (Carr) as a function of pH was studied. Experimental measurements as turbidity, hydrophobic surface, ζ-potential, and hydrodynamic size were carried out. Associative interaction between QP and Carr was found in the pH range between 1 and 2.9. When both molecules are negatively charged (pH > 5,5), a pure Coulombic repulsion regime is observed and the self-association of QP due to the Carr exclusion is proposed. In the intermediate pH range, the experimental data suggests that the charge regulation mechanism can overcome the electrostatic repulsion that may take place (and an attraction between QP and Carr can still be observed). Computational simulations by means of free energy derivatives using the Monte Carlo method were carried out to better understand the interaction mechanism between QP and Carr. QP was modeled as a single protein using one of the major proteins, Chenopodin (Ch), and Carr was modeled as a negatively charged polyelectrolyte (NCP) chain, both in the cell model framework. Simulation results showed attractive interactions in agreement with the experimental data.

1. Introduction

Foods are complex systems composed among other components of proteins and polysaccharides. These two biopolymers play an important role on the food structure, characteristics and stability due to their functional and textural properties [1]. In particular, protein in food is gaining more value due to its capacity to act on several different hierarchical structural scales from the *molecular* (where the functional properties depend directly on the protein structure) to a *mesoscale* (where the function depends on the ability of proteins to interact, form and stabilize mesostructures) and *macroscale* (where the function is an interplay of mesostructures). This new hierarchical model to define the functional properties of food proteins is based on the structural length scale required for them to achieve a particular function [2].

Starting with the molecular scale, the functional properties of proteins influence the final quality of many foods, and they depend on the structure of the proteins: particle size, hydrophobicity and zeta potential. These factors determine how the proteins interact with the solvent, with other components in the dispersion and among themselves. These parameters are altered by several conditions, such as concentration, polarity of the medium, ionic strength, presence of other components and pH [3,4].

Solubility is one of the most important factors in determining the techno-functional properties of food proteins [5]. Solubility is highly dependent on the structure of the proteins and the solution pH, and the balance between forces underlying protein-solvent and protein–protein interactions mostly determine it. This balance is affected by the pH, salt and the presence of co-solutes among others factors [5].

Here, we explore the molecular and mesoscale properties related with proteins from quinoa (*Chenopodium quinoa* Willd), a pseudocereal with high protein content and with an appropriate amino acid balance for human consumption [6]. Particularly, the quinoa protein is gaining increasing interest not only because it contains higher content of proteins than other grains but also

* Corresponding author at: University of São Paulo, School of Pharmaceutical Sciences at Ribeirão Preto, Department of Physics and Chemistry, Brazil.
E-mail addresses: flbarroso@usp.br, flbarros@ncsu.edu (F.L. Barroso da Silva).

https://doi.org/10.1016/j.ijbiomac.2017.09.076
0141-8130/

because it is a gluten-free grain [7]. Quinoa is predicted as an important future trend in the food industry. The main uses of quinoa are well reported in the literature including not only food and drinks, but also medical and repellent applications. In fact, films based on quinoa proteins and chitosan were studied as well [8].

The major quinoa seed proteins are the 11S globulin and 2S albumin (35% and 37%, respectively, of the total protein) [9]. The 11S globulin, chenopodin (Ch), has two heterogeneous sets of polypeptides, one acid (22–23 kDa) and one basic (32–39 kDa) which are joined by disulfide bonds in the native protein [10]. It is known that the acidic and basic polypeptides of 11S globulin are synthesized as one long precursor, which is later separated by proteolytic cleavage [11].

The mesoscale properties of the quinoa protein are investigated here by means of its complex formation with carrageenan (Carr), a generic name for a family of sulfated polysaccharides obtained from certain species of red seaweeds, widely used in food industry. They behave as polyelectrolytes, and are classified into three types: kappa (κ-), iota (ι-) and lambda (λ-) carrageenan. The ι-Carr is the one used in this work. It has two sulphate group per disaccharide on its backbone, leading to a pKa below 2. Carr are commonly used as stabilizers, thickeners and gelling agents in food products [12,13].

Although extensive research has been carried out on food protein–polysaccharide interactions, most has been made using milk [14] or soy proteins [12]. Despite the high potential economic interest [15], carrageenan–quinoa protein interactions have not been elucidated yet. The knowledge of the physical chemical properties of quinoa proteins (QP) and Carr and the pH effects on the interaction between them may help to improve the valorization of quinoa. This study can contribute to the understanding of pH effects on the digestibility of food products based on mixed systems as emulsions or gels. Moreover, the physical chemistry of these food systems can be analyzed and compared with previous studies contributing to enhance the understanding of food proteins and their applications in general [16].

Often, experimental and theoretical studies focus on the interaction between proteins and oppositely charged polyelectrolytes, where the main driving force is related with classical Coulombic interactions. One topic of both physical chemistry and applied special interest and less explored in the literature is the peculiar association mechanism observed for (milk) proteins-polyelectrolytes interactions in regimes where both carry likely charges, the so-called complex formation “on the wrong side of pI”. Frequently, there is a research focus on whey proteins [17,18,23,26,28,29]. The study of QP-Carr was not explored before and can contribute with more experimental data to confront theoretical views and guide the design and applications of protein functionality both in food and in pharmaceuticals.

These two open issues, *i)* the lack of data specific for the QP-Carr system and *ii)* more experiments at the wrong side of pH regime, will be discussed in this present work. Our objective is therefore to examine the influence of pH on physical chemical properties of the QP and its association with Carr. This work is focused on the use of the quinoa proteins using the QP in the food industry taking advantage of all their properties, nutritional and functional. The paper has two parts: experimental and simulations following the order: applied experimental methodology, the theoretical modeling, experimental results, simulations data and discussion.

2. Materials and methods

2.1. Materials

Quinoa partially defatted flour was purchased from Los Andes (Cochabamba, Bolivia). Content for 100 g flour: 7.25 g humidity, 12.5 g proteins, 3.88 g fat, 74.2 g carbohydrates (being 2.6 g raw fibers) and 2.17 g ash (being 93.99 mg calcium, 403.93 mg phosphorus and 0.521 mg iron). ι-Carr were purchased from Sigma (Sigma Chemical, St Louis, MO, USA). The rest of the chemical reagents had analytical quality.

2.2. Quinoa protein isolation and quantification

Quinoa protein isolate (QPI) was prepared using partially defatted, solvent-free, quinoa flour provided as starting material. Aqueous alkaline (pH 8) protein extract was precipitated at pH 4.5, resuspended and solubilized at pH 8 in distilled water at a protein concentration of 5% w/w. Dispersion was frozen (−80 °C) and lyophilized.

The protein quantification of stock solutions of QPI was carried out by Bradford method and the dilutions required for each experiment were made before use.

2.3. Turbidity measurements versus pH

The turbidity of QP (0.05% w/w), Carr (0.04% w/w) and QP (0.05% w/w) + Carr (0.04% w/w) was analyzed using a UV/visible spectrophotometer at 600 nm (Jasco V550), measured versus pH. The pH variations of the medium were obtained by adding 0.5 M HCl to initial alkaline solutions and allowing the system to equilibrate before measuring the turbidity.

2.4. Protein solubility profile

Protein solubility as a function of pH was determined on QP 1.0% w/w and on mixed systems containing Carr 0.1% w/w in buffer 10 mM Acetate–10 mM Phosphate–10 mM Tris HCl (Ac-Pi-Tris). Water dispersions were stirred for 1 h at room temperature and pH was adjusted to the desired value with 0.5 N HCl or NaOH. Dispersions were centrifuged at 10000*g* for 10 min at 4 °C, and protein content was measured by Bradford [19]. Solubility was expressed as a percentage (g of soluble protein/100 g of isolate in sample). All solubility determinations were performed in triplicate.

2.5. Particle size and charge measurements

Particle sizes and charges were determined using a dynamic light scattering device (Nano Particle Analyzer Horiba SZ-100). Particle size is reported as the Z-average mean diameter or hydrodynamic diameter (D_h) and the particle charge is reported as ζ-potential (ζ), it was calculated by Helmholtz-Smoluchowski equation directly by the instrument software [20]. Samples measured were QP (0.05% w/w), Carr (0.04% w/w) and mixed systems (0.05% w/w QP + 0.04% w/w Carr), determined at 25 °C in the pH range between 1–9 with a laser of 532 nm as light source (10 mW). Water viscosity and refraction index were considered 0.000891 kg/m·s and 1.33, respectively. Values of ζ and D_h were determined in quintuplicate.

2.6. Surface hydrophobicity (S_0)

The effect of pH on the relative surface hydrophobicity of the mixed systems (QP + Carr) respect to the samples containing only QP or Carr was determined using the fluorescent probe 1-anilino-8-naphtalene-sulfonate (ANS) [21]. Aliquots of each sample were added to a 3 mL of buffer solution containing a final ANS concentration of 2 μM. Fluorescence intensity (FI) was measured with an Aminco Bowman Series 2 spectrofluorometer, at wavelengths of 365 nm (excitation) and 484 nm (emission). The initial slope (m) of FI vs. biopolymer concentration plot was used as an index of protein

hydrophobicity (S_0). All determinations were performed in triplicate. The value of the relative S_0 of the QP-Carr mixed systems was calculated, at each pH, as follows:

$$\text{Relative}S_0 = (m_{QP+Carr} - m_{Carr})/m_{QP} \quad (1)$$

being $m_{QP+Carr}$, m_{Carr} and m_{QP} the initial slope corresponding to the addition of mixed systems (QP + Carr), only Carr and only QP to the ANS solution, respectively.

3. Theoretical modeling

Since the landmark work of J.T.G. Overbeek [22], different theoretical approaches from analytical theories to computer simulation works were used to explain the protein-polyelectrolyte complex formation [18,23]. For systems with opposite charges (e.g. a positively charged protein attracting a negatively charged polymer), the main driven force is clearly the ordinary Coulombic attraction. More instigating and challenging is the association of likely-charged objects that do not follow this basic and well-known rule. At the beginning, it was frequently argued that apparently paradoxical formation of soluble complexes at conditions where the net charges of the protein and the polyelectrolyte have the same sign was due to "charged patches" on the protein surface [24,44]. However, the Kirkwood and Shumaker (KS) theory from 1952 [25] indicated that this association could be due to a special mechanism related with the proton fluctuation that result in pure electrostatic *attractive* force. Mutual rearrangements of the distributions of the charged groups as a consequence of the perturbations in the acid-base equilibrium leads to these fluctuations. They are measured by a protein property called capacitance (or the "charge fluctuation parameter"), defined mathematically as [23,26,27].

$$C = Z^2 - Z^2 \quad (2)$$

where Z is the valence (or charge number) of the protein in a given configuration, salt concentration and solution pH. The brackets <> indicate mean values and reflect the fact that amino acids can be protonated at some time, and deprotonated in another time due to the interplay of all physical interactions [26,27]. Experimentally, C can also be quantified as

$$C \propto \frac{dZ}{dpH} \quad (3)$$

Following the KS theory, the free energy of interaction [$A(R)$] between two charged objects (proteins, polyelectrolytes,. . .) A and B as a separation distance R at a very diluted salt condition is given by

$$\frac{A(R)}{kT} \approx \frac{l_B\langle Z_A\rangle\langle Z_B\rangle}{R} - \frac{l_B^2}{2R^2}\left(C_A C_B + C_A\langle Z_B\rangle^2 + C_B\langle Z_A\rangle^2\right) \quad (4)$$

where k is the Boltzmann constant (k=1.3807 × 10^{-23} J mol^{-1} K^{-1}), T is the temperature (in Kelvin) and l_b is the Bjerrum length [l_b=$e^2/4\pi e_0\varepsilon_s kT$, where e, ε_0, and ε_s correspond to, respectively, the elementary charge ($e = 1602 \times 10^{-19} C$), the vacuum permittivity (ε_0=8854 × 10^{-12} C^2/Nm^2) and the solvent dielectric constant]. The first term of this equation accounts for the usual monopole electrostatic contributions, being repulsive for likely-charged objects, and attractive for oppositely charged bodies. Conversely, the second term is always attractive and strongly dependent on this intrinsic capacity of the protein to fluctuate its net charge as a function of pH. Salt screens both terms, and it is more severe with the second one, as discussed before [28,29]. The KS theory was later tested and confirmed by computer simulations [23,26,30–32,45]. This charge regulation theory has been successfully used to explain milk protein-pectin interactions [23,26,31,32,45], protein–protein complex formation [33] and protein-nanoparticle association [29].

In order to understand the molecular mechanism of complex formation between QP-Carr, similar computer experiments of pairs of QP and Carr in an electrolyte solution at several solution pHs were performed here. Invoking a minimum set of parameters, the used molecular model was described in details in refs. [26,31,32]. Following the same model, the protein is assumed to be a rigid object, fixed at the center of a spherical simulation cell in the presence of mobile ions (counterions and salt) and described by a collection of charged hard-spheres of radius R_i modeling its atoms. Normally in such simulations, the protein atomic coordinates are taken from either crystallographic or NMR structures when available. However, there are no three-dimensional data available for Ch. Instead, a simple cartoon of this protein was produced in order to help to rationalize some of the main electrostatic phenomena. This hypothetical representation of Ch was generated based only on a geometric criterion and the protein primary sequence [34]. No protein structure algorithm was employed [46]. A more realistic approach would involve the full coupling between protonation/deprotonation and the configurational changes which requires a non-rigid model for the protein. Nevertheless, it is well-known that these flexible protein models in constant pH simulations have very slow convergence studying individual molecules [35] and this CPU cost would become prohibitive for protein-polyelectrolyte systems considering the present development status of these models. Conversely, the simplified cartoon model captures the main electrostatic properties of the system as successfully demonstrated before [26,31,32,45]. Anisotropic electrostatic interactions are partially incorporated through the generation of several random structures. In this work, five random structures for Ch were created constraining all its amino acids inside a sphere of diameter equals to 40 Å (R_p = 20 Å). Both the linear protein sequence and the peptide bond lengths were respected in the model construction process. Each generated random protein structure has a different dipole moment because of their specific amino acid three-dimensional spatial arrangement. The ionizable amino acids charges are allowed to adjust and fluctuate as a function of the pH following the same titration scheme used before [26,31,32].

The surrounding electrolyte solution was modeled by charged hard-spheres of radius 2.15 Å. These mobile particles are free to move inside the simulation cell of radius R_{cell}. Counter-ions were added in the system to respect the electroneutrality condition. All particles are kept inside the spherical box via an external potential [$U^{ext}(r_i)$]:

$$U^{ext}(r_i) = \begin{cases} 0, \text{ for } (R_i + R_P) \le r_i \le R_{cell} \\ \infty, \text{ for all other cases.} \end{cases} \quad (5)$$

Each two sites i and j (a protein charged atom, a free ion or a polymer bead) with charge numbers Z_i and Z_j spatially separated by a distance $r_{ij} > R_i + R_j$ contributes with the electrostatic potential energy [$U^{ele}(r_{ij})$] simply by the classical Coulomb potential:

$$U^{ele}\left(r_{ij}\right) = \frac{Z_i Z_j e^2}{4\pi\varepsilon_0\varepsilon_s r_{ij}} \quad (6)$$

Due to the proton titration scheme in this constant-pH simulation, the protein charges are a function of pH and can vary during the calculation, i.e. protein amino acids can either be at the protonated or deprotonated states during the simulation. For instance, arginine can have its charge equal to zero (deprotonated) or one (protonated) during the sampling, depending on the solution pH, the protonate states of other titratable sites and the salt concentration. In the presence of the polyelectrolyte, the electrical field produced by its charged fields can also affect the protonation states of all amino acids.

When $r_{ij} \leq R_i + R_j$, it is necessary to prevent the Coulombic collapse and also to model the characteristic repulsion given by the overlap of atomic electron clouds (the Pauli exclusion principle). This is often done via the hard-sphere potential [$U^{hs}(r_{ij})$]:

$$U^{hs}\left(r_{ij}\right) = \begin{cases} \infty, \text{ for } r_{ij} \leq \left(R_i + R_j\right) \\ 0, \text{ in all other conditions.} \end{cases} \quad (7)$$

Combining these expressions, we can define the total configurational energy [$U(\{\boldsymbol{r}_k\})$]:

$$U\left(\left\{\boldsymbol{r}_{\boldsymbol{k}}\right\}\right) = \sum_{i=1}^{N_c+N_s} U^{ext}\left(r_i\right) + \frac{1}{2}\sum_{i=1}^{N}\sum_{j=1}^{N}\left[U^{ele}\left(r_{ij}\right) + U^{hs}\left(r_{ij}\right)\right] \quad (8)$$

where N_c and N_s correspond to the number of counterions and added salt, respectively. The total number of charges is given by $N = N_c + N_s + N_P$, where the number of protein charged atoms (N_P) is also included.

Emulating refs [26,31,32], the Carr structure was modeled by a single flexible polyelectrolyte chain of $N_{mom} = 21$ negatively charged hard spheres of radius $R_{mon} = 2.15$ Å. The number of charged beads for the polyelectrolyte was chosen based on a reasonable trade-off between realism and sampling efficiency. For the sake of simplicity, Carr is assumed to be fully protonated in all the experimental range ($Z_{mom} = -1$) and a non-titratable object ($C_{mom} = 0$). This is a small approximation since its pKa < 2. When the polymer chain was present in the simulation box, the bond interaction potential [βU^{bond}] between neighboring beads is given by

$$\beta U^{bond} = \frac{l_b}{2r_{min}^3}\sum_{i=1}^{N_{mon}-1}\left(r_{i,i+1}\right)^2 \quad (9)$$

where $\beta = 1/(kT)$, $r_{i,i+1}$ is the spatial separation distance between the beads i and $i+1$, and $r_{\min}$ is the separation distance corresponding to the energy minimum for a dimer. As in previous works, it was assigned a value of $r_{min} = 4$ Å, which results in an average bead–bead separation of approximately 7.4 Å that reflects the electrostatic interactions between all charged monomers and the thermal fluctuations.

The standard Metropolis Monte Carlo (MC) method [36]. with random translational displacements of all mobile species [added salt, counter-ions and polyanion beads (when present in the simulation box)] within the electroneutral cell (R_{cell}=300 Å) was used to generate the configurations for analyses. Different sets of simulations were used: (a) set A – protein in an electrolyte solution (without the polymer chain), and (b) set B – a pair of a protein and a polyelectrolyte chain in an electrolyte solution. For both sets, simulations were performed in a semi-grand canonical ensemble for the five random Ch structures following the protocol described before in previous papers [26,31,32]. Salt concentration was 10 mM, and the solution pH was in the range between 1 and 11. At least 10^8 MC simulation cycles were carried out for the equilibration and production runs. During the production, physical chemical properties [the averaged net protein charge number (Z_P), the averaged protein charge regulation parameter (C_P) and the averaged protein dipole number (μ_P)] and free energy derivatives were measured at each experimental condition.

4. Results and discussion

4.1. Turbidimetric and solubility

Turbidimetric measurements are particularly useful to study aqueous systems composed by proteins and charged polysaccharides (as Carr) in order to determine if they phase-separate.

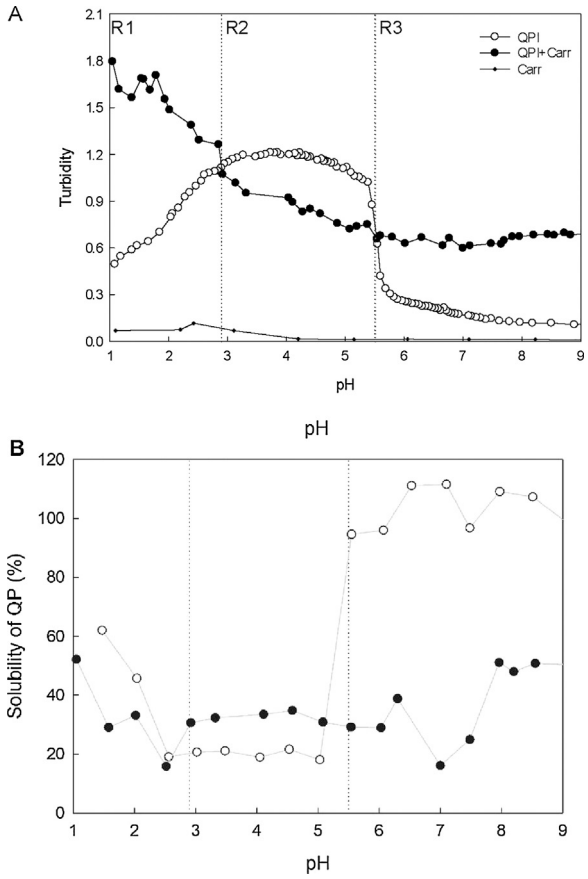

Fig. 1. A) Turbidimetric behavior of the systems composed by QP 0.05%w/v, Carr 0.04%w/v and QP 0.05%w/v + Carr 0.04%w/v at different pH. Turbidity was determined as absorbance at 600 nm. B) Solubility of QP 1%w/v, expressed as percentage, in the absence and the presence of Carr 0.04%w/v. Medium: Ac-Pi-Tris 10 mM. Temperature: 25 °C.

Homogeneous systems are characterized by low values of turbidity and the increase in turbidity in this type of mixed systems is often related to coacervation, precipitation or flocculation [37].

Fig. 1(A) shows the pH-dependence of the turbidity of QP and QP+Carr in an Ac-Pi-Tris 10 mM medium. The profile of turbidity obtained for QP is the typical plot corresponding to vegetable proteins that can be precipitated at its isoelectric pH. As can be observed, turbidity of QP has a maximum between solution pH 2.9 and 5.5, range which is known to correspond to the lesser solubility of these proteins (in fact, the QP was obtained by protein precipitation at this pH range). This turbidity diagram shows that the pH range studied could be divided into three relevant regions, from left to right: **R1)** the acid region, **R2)** the region corresponding to the isoelectric precipitation of QP, and **R3)** the neutral-alkaline region.

In the R1 region, the turbidity of the QP+Carr systems is higher than the turbidity of the systems containing only QP; and the turbidity increases as the medium becomes more acid. This could be suggesting that QP and Carr are interacting, probably electrostatically, and forming soluble or non-soluble aggregates. In this pH range, QP and Carr carry opposite electrical charge (see below the data for the zeta potential), suggesting that an attractive Coulombic interaction may be taking place.

At the QP precipitation pH range (R2), the turbidity of the QP+Carr mixed systems is lesser than the turbidity of the QP. This could be suggesting that the presence of Carr in the system is diminishing the insolubility of QP. When the pH of the suspension for QP+Carr mixed systems is higher than the pI of the proteins, it is expected that both biopolymers carry a similar net charge.

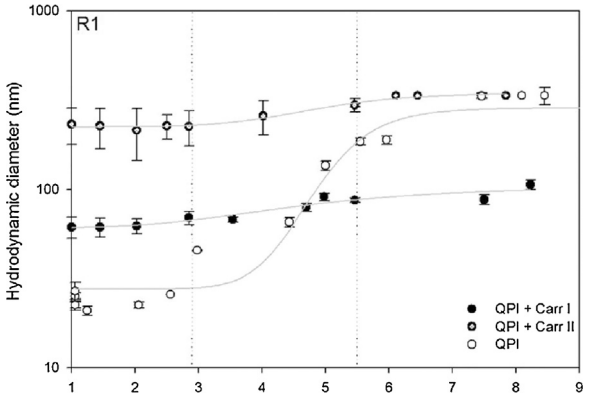

Fig. 2. Hydrodynamic diameter of the particles in systems containing QP 0.5 g/L and QP 0.5 g/L + Carr 0.004 g/L. Medium: Ac-Pi-Tris 10 mM. Temperature: 25 °C.

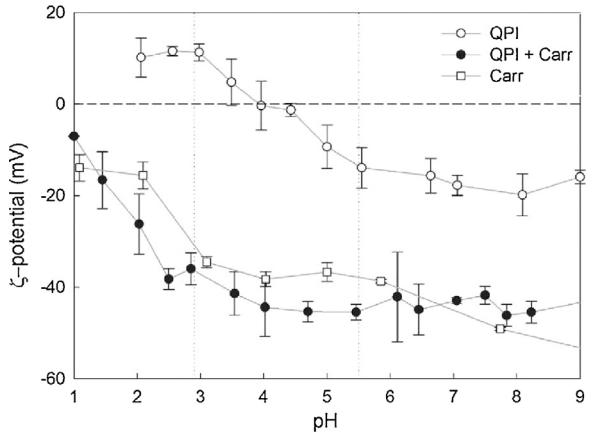

Fig. 3. ζ-potential of the particles in systems containing QP 0.05%w/v and QP + Carr 0.04%w/v. Medium: Ac-Pi-Tris 10 mM. Temperature: 25 °C.

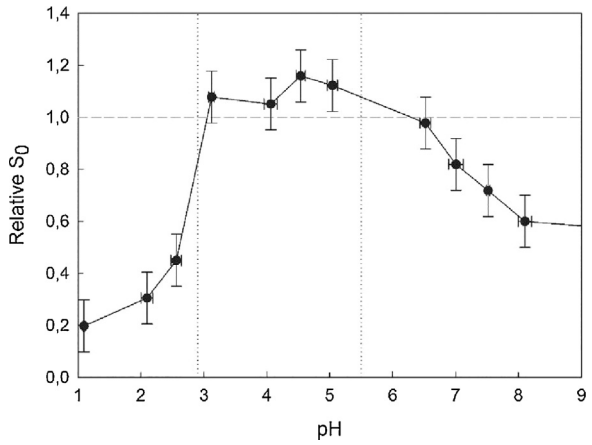

Fig. 4. Relative hydrophobicity of the particles in systems containing QP 0.05%w/v and QP + Carr 0.04%w/v. Medium: Ac-Pi-Tris 10 mM. Temperature: 25 °C.

At neutral and alkaline pH range (R3), QP+Carr mixed systems present higher optical density than those corresponding to only QP. This could be attributed to, at least, one of these two reasons: 1) the presence of Carr is diminishing the QP solubility at alkaline pH, and 2) the presence of Carr is somehow producing the aggregation of QP (either, mixed aggregates composed by QP and Carr, or QP aggregates induced by the addition of Carr).

In order to determine the effect of Carr on the solubility of the QP in the three different regions, the concentration of QP was determined both in the absence and in the presence of Carr at different pH values (Fig. 1B). In fact, as suggested in the turbidimetric experiment, the solubility of the QP was diminished in the presence of Carr in both extremes of the pH range, i.e. in the R1 and in the R3 region. However, the reason for the decrease of the QP solubility in these two regions is presumably different: i) in R1, QP and Carr would be electrostatically interacting and forming insoluble complexes, and ii) in R3, the presence of Carr could be producing the self-aggregation of the QP, probably due to the exclusion of the Carr from the QP surface, i.e., due to a depletion flocculation mechanism. On the other hand, there is a little increase in the solubility of QP in the presence of Carr in the 2.9–5.5 pH range (R2).

4.2. Hydrodynamic diameter

The hydrodynamic diameter of the structures in soluble systems composed by QP or by QP and Carr was determined by light scattering techniques (Fig. 2). The systems composed by QP shows, for the entire pH range, only one group, whose diameter increases with the increase in the pH. This can be seen in vegetable proteins because they used to form naturally aggregates at basic pH levels [38]. When Carr is also in the media, there are present two populations: I) one which size corresponds to the size of Carr in solution and II) another, of higher Dh. This group of higher sizes in the mixed systems could be assigned to aggregates of QP in the R3 region and to QP-Carr complexes in the R1 and R2 regions.

4.3. ζ-potential

QP and Carr ζ-potential were measured at different pH levels. As is shown in Fig. 3, QP ζ-potential was positive (up to +11 mV) at pH lower than 4, while at higher pH values the ζ-potential became negative (up to −21 mV). These results are in agreement with the previous results based on the turbidity measurements, where the QP isoelectric point was around pH 4.5. Carr ζ-potential was negative in all the pH range (pKa < 2) studied, which is in agreement with the presence of sulphate groups in the Carr molecule [39].

The dependence of the ζ-potential on pH of the QP+Carr systems resembles the profile of the ζ-potential of the Carr suspensions. The increase in the solubility of QP in the R2 region could be an effect of Carr presence, and insoluble QP could be solubilized due to its interaction with Carr. The association of QP with Carr produces the electrostatic repulsion between the negative charges of the QP+Carr complexes. It is worthwhile to note that we are suggesting that the complex formation is taking place at pH up to 5.5, including the range from 4.5 to 5.5 where both macromolecules carry negative charges. This corresponds to the interaction "on the wrong side of pI" as was mentioned in the Introduction section.

4.4. Surface hydrophobicity

Fig. 4 shows the dependence on the solution pH of the relative superficial hydrophobicity of the QP-Carr systems. It is remarkable that in the R2 region, the relative surface hydrophobicity (S_0) is about 1, meaning that there is no statistical difference between the S_0 of the QP and the S_0 of the QP-Carr systems. On the other hand, the relative S_0 is less than 1 in R3 region, meaning that the presence of Carr in the systems is producing a decrease in the S_0 of the QP. This hydrophobicity decrease of the QP in the presence of Carr suggests that the interactions that are taking place involve hydrophobic residues of the protein surface and are, at least partially, due to hydrophobic interactions. As it was previously discussed, the aggregates formed in the R3 region are proposed to be QP-QP, probably due to the preferential exclusion of the Carr from the protein surface.

On the other hand, the decrease in the ANS binding to the QP-Carr systems relative to the QP dispersions in the R1 may be not only related with the change in the hydrophobicity but also with the change in the superficial charge of the particles. The ANS molecule is negatively charged and its charge is probably responsible for some degree of electrostatic interaction to the positively charged QP in the R1; however, as the interaction of QP with Carr modifies the superficial charge of the particles, as is was shown above, this could be affecting the ANS binding more than the hydrophobicity of the studied systems.

4.5. Theoretical data

Numerical simulations can provide quantitative insights into the relevant molecular mechanisms that are driven the protein-polyelectrolyte interaction at all solution pH levels [23,26,31,32,45]. A quantitative and completely detailed way to describe QPI–Carr would be quite difficult because the QPI is not fully characterized and the full description of Carr would require prohibitive high CPU costs. Previous studies of Brinergar [9,10] have shown that the 34% of the QPI consists of Ch, for which the mRNA sequence is known and available. Therefore, for the sake of convenience, molecular simulations can follow a simplified route and concentrate on Ch. This leads to a semi-qualitatively description of the physicochemical interactions between one of the major proteins contained in the isolate, Ch, and a NCP simplified as a set of negative charged spheres connected by a harmonic spring model.

In the experimental section above, combining the different experimental measurements, three different pH regions are identified: a) *R1*: pH $\leq$ 2.9, where Coulombic attractive forces between the negatively charged Carr and the positively charged QPI favors the formation of QPI-Carr complexes; b) *R2*: 2.9 < pH < 5.5, where the experimental data suggest that the charge regulation mechanism can overcome the electrostatic repulsion that may take place (and an attraction can still be observed); c) *R3:* pH $\geq$ 5.5, when both molecules are negatively charged, and a pure Coulombic repulsion regime is observed.

The understanding of the physical reasons for these three regions becomes clearer when combining the experimental analyses with the theoretical approach. From the computer simulations, the titration plot given in Fig. 5A indicates a pI equals to 6.9 for the hypothetical Ch model which is higher than the pI for the QPI (pI estimated to be 4.5) [40]. In the literature, values in the interval of 5.0–6.5 are found [6]. This computed titration behavior was obtained for a system with a single Ch molecule in an electrolyte solution (the polyelectrolyte was absent in this set of calculations). The errors bars indicate that the five random models give similar results for pH values closer to the pI. The smallest errors are observed at pI indicating that the random models are not affecting its prediction. In fact, as demonstrated before, pI can be reasonable well estimated from the polypeptide amino acid composition [41].

The discrepancy between the theoretical and experimental data might be a result of the discrepancy of the simulation and the experimental conditions. Moreover, Ch was assumed to be able to describe the experimental behavior of QPI. The error bars increase as pH departs from the pI in both acid and basic regimes. This implies that at these pHs, protein conformation has a marked effect on the titration. Based on this data (and assuming only monopole electrostatic interactions), the Coulombic attractive regime should be observed for pH < 6.9. At pH > 6.9, where both protein and polyelectrolyte are negatively charged, Coulombic repulsive forces would make the complex formation impossible.

A similar plot for the protein charge regulation parameter varying with pH is given in Fig. 5B. This protein property varies with pH as a consequence of the number of amino acid residues that titrate around each pH. Since charge fluctuations are largest when

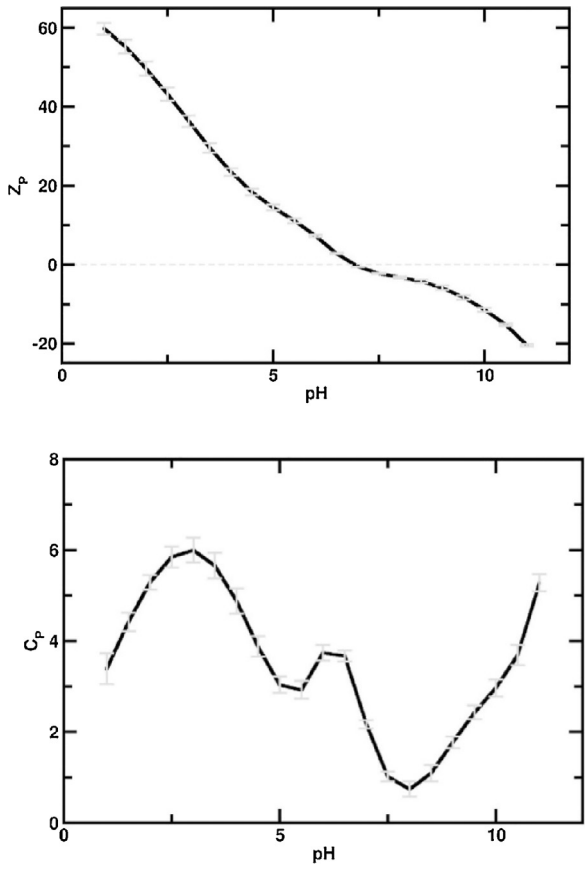

Fig. 5. A) The simulated averaged charge number of the protein Ch as a function of pH. The salt concentration is 10 mM and the protein concentration is 58.7 mM. Data from the five random Ch structures was averaged. The corresponding estimated deviations are illustrated in the plot with error bars. B) The simulated averaged charge regulation parameter of the Ch as a function of pH. The salt concentration is 10 mM and the protein concentration is 58.7 mM. Data from the five random Ch structures was averaged. The corresponding estimated deviations are illustrated in the plot with error bars.

pH $\approx$ pKa of a certain residue, C_P of a protein rich in say, glutamic acid will peak at pH 4.4 [pKa_{glu} = 4.4 [42]]. Higher values of C_P indicate conditions where the *attractive* electrostatic interactions predicted by KS are also higher (Kirkwood & Shumaker) [25]. In general, the C_P values for Ch are larger than observed for several other food proteins [25,32]. Around pH 7, $C_P \approx 2$ which, as seen by Eq. (4), can contribute to non-negligible attractive interactions. From this data, it can be anticipated the QPI-Carr complex formation on the wrong side of pI due to the (always attractive) charge regulation contribution, supporting the experimental data.

All the three regimes were identified by the computed radial distribution functions [$g(r)$] as a function of the separation distance (r) for the polymer beads-protein center – see Fig. 5(A). It becomes easier to see these regimes plotting $g(r)\cdot r^2$ as a function of r. This plot enhances the possible regimes: a) at acidic pH, Coulombic attraction due to the oppositely charges between QPII and Carr; b) intermediate pH range, attraction due to the charge regulation mechanism [including the so called "complex formation of the wrong side of pI" – in this case, pI = 6.9 as seen in Fig. 5A], and (c) at alkaline pH Coulombic repulsion are the dominant driving force prohibiting the QPII-Carr complex formation. The sharp peaks observed at the Coulombic attractive condition becomes lower as pH is increased to the basic regimes. Peaks become smaller and narrower. Fig. 6 identifies that the electrostatic attraction around pI for pH > pI is not so tightly as observed for pH $\ll$ pI. This indicates that part of the polyelectrolyte is in contact with the protein

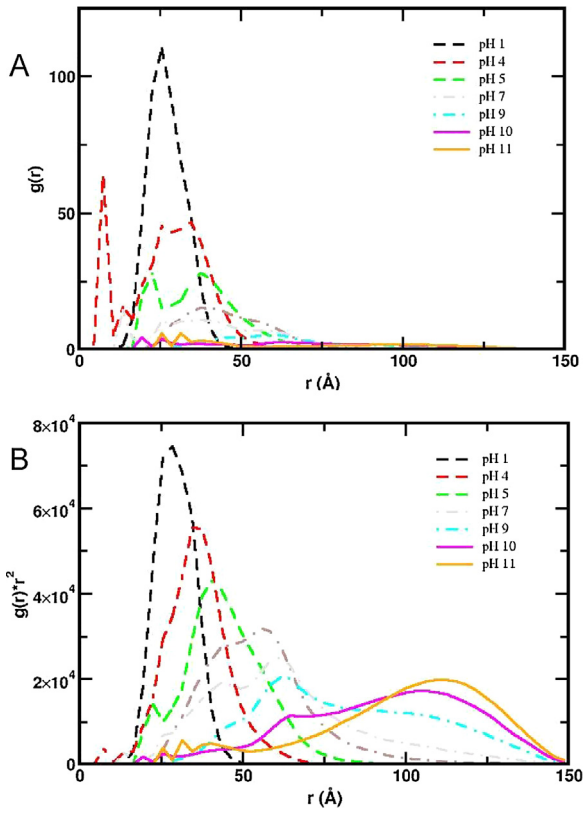

Fig. 6. Computed free energy derivatives as a function of the separation distance between the protein center and the polyelectrolyte beads at 10 mM of salt at different solution pHs. (A) radial distribution function [g(r)]. (B) $g(r)\cdot r^2$. Data from the five random Ch structures were averaged. Different lines represent each regime: dashed (Coulombic attraction), dashed-point (attraction due the charge regulation mechanism) and solid (Coulombic repulsion).

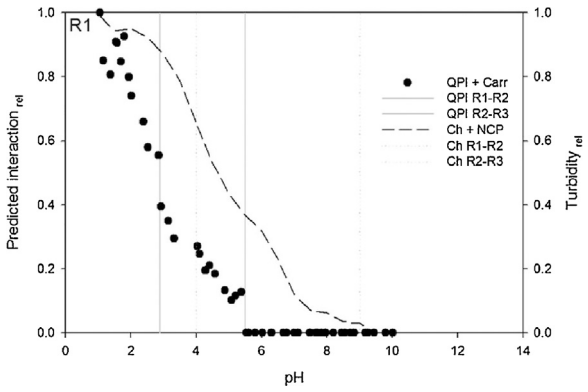

Fig. 7. Effect of pH on the experimental interaction between QPI and Carr (•) and on the simulated interactionbetween Ch and NCP (black lines). Experimental regions defined by continue lines (_). Simulations regions defined by dots (. . .).

surface while another part of the chain is floating separated of the surface in the electrolyte solution. Indeed, the KS predicts an attraction shorter in the range ($1/r^2$) when compared to the longer range Coulombic interaction ($1/r$).

4.6. Experimental and computational results comparison

In order to *qualitatively* compare the experimental results and the theoretical simulations, relative magnitudes quantifying the interaction were defined and showed in Fig. 7:

- Turbidity_{rel} = (higher turbidity value observed – lower turbidity value observed)/higher turbidity value observed
- $\text{Predicted interaction}_{rel}$ = (higher free energy derivate observed-lower positive value observed)/higher free energy derivate observed.

From the five Ch 3D models by randomization were made and, the interaction between Ch and NCP was quantified by means of free energy derivatives from the radial distribution function from the separation distance between both mass centers. The results presented in Fig. 7 are the average from the five random forms of Ch calculated.

5. Conclusion

Quinoa protein is an important trend in the industrial scenario that still needs more research studies. Its interactions with food polyelectrolytes is one of the properties that requires more understanding to support commercial applications. This was the main problem investigated here as a function of solution pH. Different complex formation regimes could be identified for the QPI-Carr system. There are three distinct regions observed both by the experimental and simulated results as showed in Fig. 7. They are characterized by ordinary Coulombic interactions and the peculiar charge regulation mechanism.

It is noted that despite the pH values of the limits of these regions differing in each approach, there is an agreement in the observed behavior. The limit between regions 1 and 2 (from pure attractive Coulombic interaction to the charge regulation interaction regime) takes place when the relative interaction magnitude is around 0.6. The limit between R2 and R3 (from the charge regulation mechanism regime to the repulsive interaction regime) was identified as the pH at which the relative interaction magnitude became null.

The quantitative differences between the region limits can be assigned to many factors such as: the sensitivity of turbidimetry methods not comparable with the simulations results accuracy, QPI is not fully characterized by the approximated hypothetical model adopted for Ch, the flexible chain model used for Carr, the lack of both the hydrophobic effect (due to the use of a continuum solvent model) and other interactions such as protein–protein since only a single pair of protein- polyelectrolyte was simulated. The latter is directly related with the different hierarchical scales between the experimental (mesoscopic scale) and simulated (molecular scale) conditions. The simulation would just allow explaining the physical- chemical factors affecting this process in the experiments, in spite of their intrinsically limitations.

However, the simulations allow qualitative characterization of the interaction between QPI and Carr, explaining the experimental findings and contributing to the understanding of the molecular mechanisms behind the experimentally observed quantities. The charge regulation mechanism often seen in biological and biotechnological systems [23,26,27,29,31,32,43,45] was again observed for another food protein system. This contributes to demonstrate how general and important this mechanism is despite it being relatively new in the food protein literature.

Acknowledgements

This work has been supported in part by the Consejo Nacional de Investigaciones Científicas y Técnicas (CONICET), Agencia Nacional de Promoción Científica y Tecnológica (PICT 2014-1571), Universidad Nacional de Rosario (BIO385, BIO430), Fundação de Amparo à Pesquisa do Estado de São Paulo [Fapesp – Grant no. 2015/16116-3 (FLBDS)], the University Global Partnership Network (UGPN) Research Collaboration Fund (FLBDS) and the University College

Dublin (UCD) through a visiting professors grant - Seed Funding (FLBDS). FLBDS thanks also the support of the University of São Paulo through the NAP-CatSinQ (Research Core in Catalysis and Chemical Synthesis), the computing hours at Rice University through the international collaboration program with USP and at The Swedish National Infrastructure for Computing (SNIC 2015/10-6), and the hospitality of UCD, Ireland. We thank Martha Zepeda Rivera from Harvard University, Massachusetts, United States, for English correction in the manuscript.

References

[1] C. Schmitt, S.L. Turgeon, Protein/polysaccharide complexes and coacervates in food systems, Adv. Colloid Interface Sci. 167 (2011) 63–70, http://dx.doi.org/10.1016/j.cis.2010.10.001.
[2] E.A. Foegeding, Food protein functionality–a new model, J. Food Sci. 80 (2015) C2670–C2677, http://dx.doi.org/10.1111/1750-3841.13116.
[3] K. Nishinari, Y. Fang, S. Guo, G.O. Phillips, Soy proteins: a review on composition, aggregation and emulsification, Food Hydrocoll. 39 (2014) 301–318, http://dx.doi.org/10.1016/j.foodhyd.2014.01.013.
[4] S.M.H. Hosseini, Z. Emam-Djomeh, M. Negahdarifar, M. Sepeidnameh, S.H. Razavi, P. Van der Meeren, Polysaccharide type and concentration affect nanocomplex formation in associative mixture with β-lactoglobulin, Int. J. Biol. Macromol. (2016), http://dx.doi.org/10.1016/j.ijbiomac.2016.09.037.
[5] S. Benelhadj, A. Gharsallaoui, P. Degraeve, H. Attia, D. Ghorbel, Effect of pH on the functional properties of Arthrospira (Spirulina) platensis protein isolate, Food Chem. 194 (2016) 1056–1063, http://dx.doi.org/10.1016/j.foodchem.2015.08.133.
[6] O.E. Mäkinen, E. Zannini, P. Koehler, E.K. Arendt, Heat-denaturation and aggregation of quinoa (Chenopodium quinoa) globulins as affected by the pH value, Food Chem. 196 (2016) 17–24.
[7] A.B. Nongonierma, S. Le Maux, C. Dubrulle, C. Barre, R.J. FitzGerald, Quinoa (Chenopodium quinoa Willd.) protein hydrolysates with in vitro dipeptidyl peptidase IV (DPP-IV) inhibitory and antioxidant properties, J. Cereal Sci. 65 (2015) 112–118, http://dx.doi.org/10.1016/j.jcs.2015.07.004.
[8] L.E. Abugoch, C. Tapia, M.C. Villamán, M. Yazdani-pedram, M. Díaz-dosque, Characterization of quinoa protein and chitosan blend edible films, Food Hydrocoll. 25 (2011) 879–886, http://dx.doi.org/10.1016/j.foodhyd.2010.08.008.
[9] C. Brinegar, B. Sine, L. Nwokocha, High-cysteine 2S seed storage proteins from quinoa (Chenopodium quinoa), J. Agric. Food Chem. 44 (1996) 1621–1623.
[10] C. Brinegar, S. Goundan, Isolation and characterization of chenopodin, the 11S seed storage protein of quinoa (Chenopodium quinoa), J. Agric. Food Chem. 41 (1993) 182–185.
[11] J.W.S. Brown, D.R. Ersland, T.C. Hall, Molecular aspects of storage protein synthesis during seed development, in: The Physiology and Biochemistry of Seed Development, Dormancy, and Germination, Elsevier, 1982, pp. 3–42.
[12] I. Tavernier, A.R. Patel, P. Van der Meeren, K. Dewettinck, Emulsion-templated liquid oil structuring with soy protein and soy protein: κ-carrageenan complexes, Food Hydrocoll. 65 (2016) 107–120, http://dx.doi.org/10.1016/j.foodhyd.2016.11.008.
[13] A.K. Stone, M.T. Nickerson, Food Hydrocolloids Formation and functionality of whey protein isolate e (kappa-, iota-, and lambda-type) carrageenan electrostatic complexes, Food Hydrocoll. 27 (2012) 271–277, http://dx.doi.org/10.1016/j.foodhyd.2011.08.006.
[14] A.A. Perez, C.R. Carrara, C. Carrera, J.M. Rodríguez, L.G. Santiago, Interactions between milk whey protein and polysaccharide in solution, Food Chem. 116 (2009) 104–113, http://dx.doi.org/10.1016/j.foodchem.2009.02.017.
[15] D. Bazile, S. Salcedo, T. Santivañez, Conclusions: Challenges, Opportunities and Threats to Quinoa in the Face of Global Change, 2016.
[16] Y. Hu, J. Zhang, L. Zou, C. Fu, P. Li, G. Zhao, Chemical characterization, antioxidant, immune-regulating and anticancer activities of a novel bioactive polysaccharide from Chenopodium quinoa seeds, Int. Biol. Macromol. 99 (2017) 622–629, http://dx.doi.org/10.1016/j.ijbiomac.2017.03.019.
[17] B. Vardhanabhuti, U. Yucel, J.N. Coupland, E.A. Foegeding, Interactions between β-lactoglobulin and dextran sulfate at near neutral pH and their effect on thermal stability, Food Hydrocoll. 23 (2009) 1511–1520, http://dx.doi.org/10.1016/j.foodhyd.2008.09.006.
[18] T. Wagoner, B. Vardhanabhuti, E.A. Foegeding, Designing whey protein-Polysaccharide particles for colloidal stability, Annu. Rev. Food Sci. Technol. 7 (2016) 93–116, http://dx.doi.org/10.1146/annurev-food-041715-033315.
[19] M.M. Bradford, A rapid and sensitive method for the quantitation microgram quantities of protein utilizing the principle of protein-dye binding, Anal. Biochem. 254 (1976) 248–254, http://dx.doi.org/10.1016/0003-2697(76)90527-3.
[20] R.J. Hunter, Zeta Potential in Colloid Science: Principles and Applications, Academic press, 2013.
[21] A. Kato, S. Nakai, Hydrophobicity determined by a fluorescence probe method and its correlation with surface properties of proteins, Biochim. Biophys. Acta – Protein Struct. 624 (1980) 13–20, http://dx.doi.org/10.1016/0005-2795(80)90220-2.
[22] J.T. Overbeek, M.J. Voorn, Phase separation in polyelectrolyte solutions; theory of complex coacervation, J. Cell. Physiol. Suppl. 49 (1957) 7–22, http://dx.doi.org/10.1002/jcp.1030490404.
[23] B. Jönsson, M. Lund, F.L. Barroso da Silva, Electrostatics in macromolecular solutions, in: Conf. Food Colloids, Royal Society of Chemistry, Cambridge, 2007, pp. 129–154, http://dx.doi.org/10.1039/9781847557698-00127.
[24] S. Matter, S.Y.H. Berlin, C.Y.H. Berlin, G. Charit, M.B.H. Berlin, Interaction of Human Serum Albumin with Short Polyelectrolytes: A Study by Calorimetry and Computer Simulation Interaction of Human Serum Albumin with Short Polyelectrolytes: A Study by Calorimetry and Computer Simulation, 2015, http://dx.doi.org/10.1039/C5SM00687B.
[25] J.G. Kirkwood, J.B. Shumaker, Forces between protein molecules in solution arising from fluctuations in proton charge and configuration, Proc. Natl. Acad. Sci. 38 (1952) 863–871.
[26] F.L. Barroso da Silva, M. Lund, B. Jönsson, T. Åkesson, On the complexation of proteins and polyelectrolytes, J. Phys. Chem. B. 110 (2006) 4459–4464.
[27] M. Lund, B. Jönsson, Charge regulation in biomolecular solution, Q. Rev. Biophys. 46 (2013) 265–281, http://dx.doi.org/10.1017/S003358351300005X.
[28] L.A. Delboni, F.L. Barroso da Silva, On the complexation of whey proteins, Food Hydrocoll. 55 (2016) 89–99, http://dx.doi.org/10.1016/j.foodhyd.2015.11.010.
[29] F.L.B. da Silva, M. Boström, C. Persson, Effect of charge regulation and ion – dipole interactions on the selectivity of protein – nanoparticle binding, Langmuir 30 (2014) 4078–4083, http://dx.doi.org/10.1021/la500027f.
[30] E. Dickinson, M.E. Leser, Food Colloids: Self-assembly and Material Science, RSC Pub, 2007.
[31] F.L. Barroso da Silva, Peculiaridades nos mecanismos moleculares de proteínas em solução aquosa: exemplo da importância do equilíbrio ácido-base para aplicações em biotecnología, Química (2013) 43–48 http://www.spq.pt/magazines/BSPQ/662/article/30001873/pdf.
[32] F.L. Barroso da Silva, B. Jönsson, Polyelectrolyte –protein complexation driven by charge regulation, Soft Matter 5 (2009) 2862, http://dx.doi.org/10.1039/b902039j.
[33] M. Lund, B. Jönsson, On the charge regulation of proteins, Biochemistry 44 (2005) 5722–5727.
[34] E. Kaspchak, M.A.S. de Oliveira, F.F. Simas, C.R.C. Franco, J.L.M. Silveira, M.R. Mafra, L. Igarashi-Mafra, Determination of heat-set gelation capacity of a quinoa protein isolate (Chenopodium quinoa) by dynamic oscillatory rheological analysis, Food Chem. 232 (2017) 263–271, http://dx.doi.org/10.1016/j.foodchem.2017.04.014.
[35] W. Chen, Y. Huang, J. Shen, Conformational activation of a transmembrane proton channel from constant pH molecular dynamics, J. Phys. Chem. Lett. 7 (2016) 3961–3966, http://dx.doi.org/10.1021/acs.jpclett.6b01853.
[36] N. Metropolis, A.W. Rosenbluth, M.N. Rosenbluth, A.H. Teller, E. Teller, Equation of state calculations by fast computing machines, J. Chem. Phys. 21 (1953) 1087–1092, http://dx.doi.org/10.1063/1.1699114.
[37] J. Lombardi, G. Picó, V. Boeris, Physicochemical study of the formation of complexes between pancreatic proteases and polyanions, Int. J. Biol. Macromol. 79 (2015) 160–166, http://dx.doi.org/10.1016/j.ijbiomac.2015.04.034.
[38] O.E. Mäkinen, E. Zannini, E.K. Arendt, Modifying the cold gelation properties of quinoa protein isolate: influence of heat-Denaturation pH in the alkaline range, Plant Foods Hum. Nutr. 70 (2015) 250–256.
[39] V.L. Campo, D.F. Kawano, D.B. da Silva, I. Carvalho, Carrageenans: biological properties, chemical modifications and structural analysis – a review, Carbohydr. Polym. 77 (2009) 167–180, http://dx.doi.org/10.1016/j.carbpol.2009.01.020.
[40] S.A. Elsohaimy, T.M. Refaay, M.A.M. Zaytoun, Physicochemical and functional properties of quinoa protein isolate, Ann. Agric. Sci. 60 (2015) 297–305, http://dx.doi.org/10.1016/j.aoas.2015.10.007.
[41] C.S. Patrickios, E.N. Yamasaki, Polypeptide amino acid composition and isoelectric point. II. Comparison between experiment and theory, Anal. Biochem. 231 (1995) 82–91, http://dx.doi.org/10.1006/abio.1995.1506.
[42] Y. Nozaki, C. Tanford, [84] Examination of titration behavior, Methods Enzymol. 11 (1967) 715–734, http://dx.doi.org/10.1016/S0076-6879(67)11088-4.
[43] F.L. Barroso da Silva, P. Derreumaux, S. Pasquali, Protein-RNA complexation driven by the charge regulation mechanism, Biochem. Biophys. Res. Commun. 12 (July) (2017), http://dx.doi.org/10.1016/j.bbrc.2017.07.027, pii: S0006-291X(17)31358-X. [Epub ahead of print].
[44] R. de Vries, Monte Carlo Simulations of Flexible Polyanions Complexing with Whey Proteins at Their Isoelectric, Point, J. Chem. Phys. 120 (2004) 3475–3481.
[45] D. Srivastava, E. Santiso, K.E. Gubbins, F.L. Barroso da Silva, Computationally mapping pKa shifts due to the presence of a polyelectrolyte chain around whey proteins, Langmuir (2017), http://dx.doi.org/10.1021/acs.langmuir.7b02271.
[46] C.R. Brasil, A.C. Delbem, F.L. Barroso da Silva, Multiobjective evolutionary algorithm with many tables for purely ab initio protein structure prediction, J. Comput. Chem. 34 (2013) 1719–1734, http://dx.doi.org/10.1002/jcc.23315.